

Investigation of performance of bimodal/functionalized mesoporous silica nanoparticles on the adsorption of methylene blue from aqueous solution

Shahnaz Nayyeri¹, Amir Vahid^{2*}, Majid Abdous¹, Aliakbar Miran Beigi²

¹ Faculty of chemistry, Amirkabir University of Technology, Tehran, Iran

² Research institute of petroleum industry, Tehran, Iran

Received: 2017-10-20

Accepted: 2018-02-29

Published: 2018-03-20

ABSTRACT

In this study, bimodal mesoporous silica, i.e. UVM-7, was synthesized and functionalized with sulfonic acid and characterized using XRD, nitrogen physisorption, SEM, TEM and acid/base titration. The results displayed that bimodal mesopore structure was firmly formed and acidic functional groups were grafted on the surface of the UVM-7. The concentration of the acidic functional groups was determined via titration by the standard NaOH solution. At the second step, the adsorption of methylene blue from aqueous solutions onto UVM-7 and UVM-7/SO₃H was investigated. The effect of PH, temperature, dye concentration, salt concentration and contact time on the adsorption of methylene blue was studied. The adsorption equilibrium isotherms were well fitted to Langmuir rather than Freundlich model. Methylene blue adsorption on UVM-7 increases with increasing the temperature and PH, which indicates that the process is endothermic. Maximum adsorption capacity of methylene blue by UVM-7 and UVM-7/SO₃H were 107.5 mg/g and 129.9 mg/g, respectively. The adsorption kinetics of methylene blue for both UVM-7 and UVM-SO₃H were pseudo-second order and well fitted to Langmuir model.

Keywords: Adsorption; Isotherm; Methylene blue; Mesoporous silica; Wastewater treatment.

© 2018 Published by Journal of Nanoanalysis.

How to cite this article

Nayyeri Sh, Vahid A, Abdous M, Miran Beigi AA. Investigation of Performance of Bimodal/Functionalized Mesoporous Silica Nanoparticles on The Adsorption of Methylene Blue From Aqueous Solution. J. Nanoanalysis., 2018; 5(1): 17-25. DOI: [10.22034/jna.2018.541846](https://doi.org/10.22034/jna.2018.541846)

INTRODUCTION

Color is the first contaminant to be recognized in wastewater streams. Increase in the production of paints and dyes and many uses in variety of industries leading to production of wastewater, which in turn will cause environmental pollution concerns [1,2]. Different industries such as textile, paper, pharmaceutical, food and cosmetic use dyes

and paints [3]. The presence of trace amounts of dyes in water, even lower than 1 ppm for some dyes, is unpleasant [4]. Various techniques have been employed for the removal of dyes from wastewaters. The conventional methods for treating dyes containing wastewaters are coagulation and flocculation [5-7], oxidation [8,9], membrane separation [10] and adsorption [11,12]. Adsorption technology is inexpensive and high potential in removal of small molecules, dyes and organic

* Corresponding Author Email: avahid753@gmail.com
Tel: +98(21)48255042

matter, and so one of the most efficient methods for the removal of dyes from wastewater industries than the others [13,14]. Methylene blue (hereinafter MB) is one of the most important dyes which uses in many industries and causes unclerness of water at very low concentrations because of its high adsorption coefficient. Furthermore, MB is not strongly hazardous; it can cause some harmful effects if there is too much such as increased heart rate, vomiting, shock, cyanosis and tissue necrosis in human [5-7]. Various types of adsorbent such as zeolites, mesoporous silicas, activated carbon, clays and nanomaterials have been investigated for removing dyes from aqueous solution [15]. In recent years, nanosize bimodal mesoporous silica, i.e. UVM-7, was synthesized. This mesoporous material with high surface area and bimodal porosity can be combined with functional chemical groups for the removal of pollutants from the environment [16].

In this study UVM-7 synthesized and functionalized with SO_3H and used for the absorption of cationic dye, i.e. MB. The effect of different parameters such as PH, temperature, contact time, salt concentration and initial dye concentration was studied. The equilibrium adsorption data were fitted to Langmuir and Freundlich equations to determine the correlation between the experimental data and models.

EXPERIMENTAL

Materials and methods

The reactants used in this study were cetyltrimethylammonium bromide (CTAB), tetraethyl orthosilicate (TEOS) as silica source, triethanolamine (TEAH3), hydrochloric acid (HCl), Sodium hydroxide) NaOH) and MB as adsorbent. Methylene blue ($\text{C}_{16}\text{H}_{18}\text{N}_3\text{SCL}$) is a cationic blue dyestuff with Cl classification Number of 52015 and its chemical structure is shown in Figure 1.

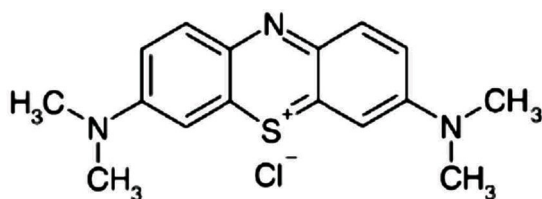


Fig. 1. Chemical structure of methylene blue dye.

Synthesis of UVM-7

The general procedure for the synthesis of UVM-7 is the atrane route, in which the presence of polyalcohol is the key to balancing the hydrolysis and condensation reaction rates [18]. In a typical synthesis, TEOS was added in determined amounts of TEAH3. The solution was heated up to 140°C under vigorous stirring. After cooling down to 90°C , CTAB was added to this solution. After that, water was added slowly to the solution under stirring until a white suspension resulted. This suspension was aged four hours at room temperature. The solid was filtered, washed with sufficient amounts of water and acetone and dried in oven at 80°C overnight. The final molar composition of the reactants was 1.0 TEOS: 3.5 TEAH3: 0.25 CTAB: 90 H_2O . Thermocalcination of the as synthesized UVM-7 was carried out under a flow of air up to 550°C for 6 hours with a heating rate of $1^\circ\text{C}/\text{min}$ to remove both the surfactant and TEAH3 from the as-synthesized UVM-7.

Synthesis of UVM-7/ SO_3H

For the functionalization of the synthesized UVM-7 with sulfonic acid groups, predetermined amount of $\text{C}_9\text{H}_{22}\text{SO}_3\text{Si}$ and 2 g of calcined sample were added to 100 mL of toluene and stirred for 24 hours at 80°C , followed by filtering and washing with proper amounts of ethanol. Then, SH group was oxidized to SO_3H via oxidation using H_2O_2 (30 %) followed by a proton exchange using HNO_3 (1 molar). 1 grams of the obtained solid was added to 100 mL water and was titrated by 0.02 molar solution of NaOH and the obtained acid concentration was 1.5 mmol/g.

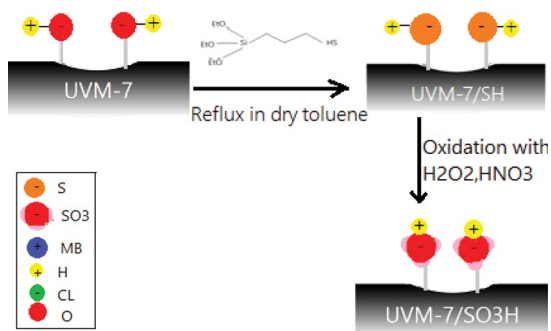


Fig. 2. Mesoporous silica functionalized with sulfonic acid.

Adsorption experiments

The solution of MB at a concentration of 200 mg/L of distilled water was prepared then diluted to the required solution) 50 ·100·150 mg/L) were converted. The concentration of MB in the supernatant solution before and after the adsorption was determined by Uv -Vis spectrometer. The absorption of the colored solution measured at a wavelength 664 nm to a calibration curve between dye concentration and absorption is drawn. Using calibration curve amount of dye adsorption by UVM-7 after each test according to the amount of absorption in the wavelength 664 nm was calculated. 10 mg of silica UVM-7 was mixed with 10 ml of the aqueous solutions of various initial concentrations (50, 100, 150, 200 mg/g) of MB. The initial PH (4, 6, 8, 10 and 12) of the solutions was adjusted with 0.5 mol/l HCl or 0.5 mol/l NaOH solutions. The flasks with their contents were shaken for the different adsorption times (20, 40, 60, 80, 100 and 120 min) at temperatures 25, 30, 35 and 40°c. The adsorbing capacity of methyl blue was calculated from the formula:

$$q_t = \frac{(c_0 - c_t)V}{M} \tag{1}$$

Where C_0 and C_e (mg/g) are respectively the initial and equilibrium concentrations of dye, V (L) is the volume of the solution and M (g) is the mass of adsorbent used.

RESULTS AND DISCUSSION

Characterization of UVM-7 and UVM-7/SO₃H

XRD patterns of UVM-7 and UVM-7/SO₃H are shown in Figure 2a–b, respectively. A strong diffraction peak can be seen in all XRD patterns which is characteristic of this type of nanoparticulated meso/ macroporous material. However, this strong peak can be attributed to diffraction from the d_{100} plane and is accompanied by a broad diffraction peak at higher angles in both samples. These broad peaks might be assigned to d_{110} and the overlap of d_{200} and d_{210} diffraction peaks on the basis of hexagonal symmetry [19,20].

Figure 4a–b illustrates the nitrogen isotherms of UVM-7 and UVM-7/SO₃H, respective Textural properties of both samples are given in Table 1. Isotherms of both samples display two distinct regions at medium and high relative pressures, which can be attributed to the presence of a bimodal pore system. The inflection at medium relative pressure corresponds to a type IV isotherm, which is typical of mesoporous

materials and suggests the presence of a well-ordered array of small mesopores in all samples. However, after the functionalization of UVM-7, the sharpness of this region decreases, which means a reduction of structural order [20].

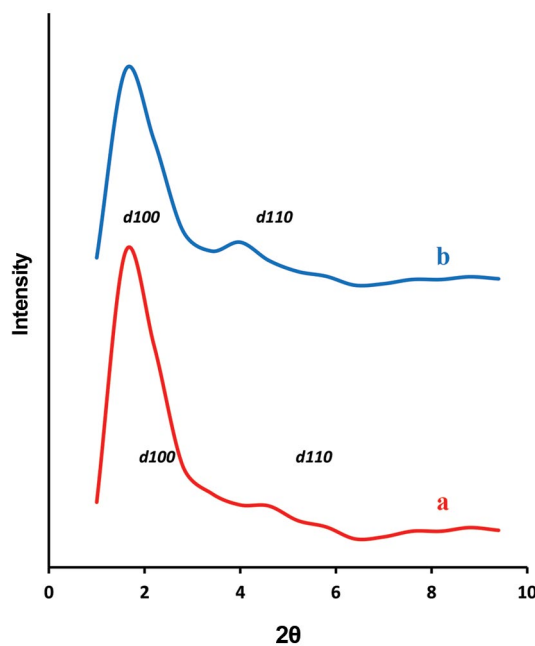


Fig. 3. XRD pattern of a) UVM-7 and b) UVM-7/SO₃H.

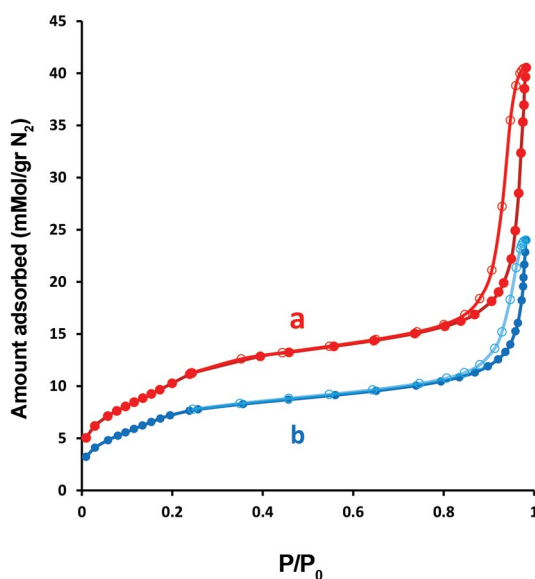


Fig. 4. Adsorption isotherms of nitrogen at 77 K on a) UVM-7 and b) UVM-7/SO₃H

Table 1. Textural properties of UVM-7 and UVM-7/SO₃H

Sample name	BET surface area (m ² /g)	Total pore volume, (m ³ /g)	Average pore volume, (nm)
UVM-7	810	0.65	33
UVM-7/SO ₃ H	416	0.33	21

Electron microscopy is a useful technique for the direct elucidation of the morphology, as well as the particle size of the nano materials. SEM image UVM-7 is illustrated in Figure 5b. It can be clearly seen, UVM-7 is formed from very small nanoparticles which are also very homogeneous in size.

TEM image of UVM-7 in Figure 5a displays small intraparticle mesopores related to the porogenic effect of the surfactant are obvious. The continuous nanometric structures constructed from these nanoparticles generate a hierarchic non-ordered system of large (interparticle) mesopores.

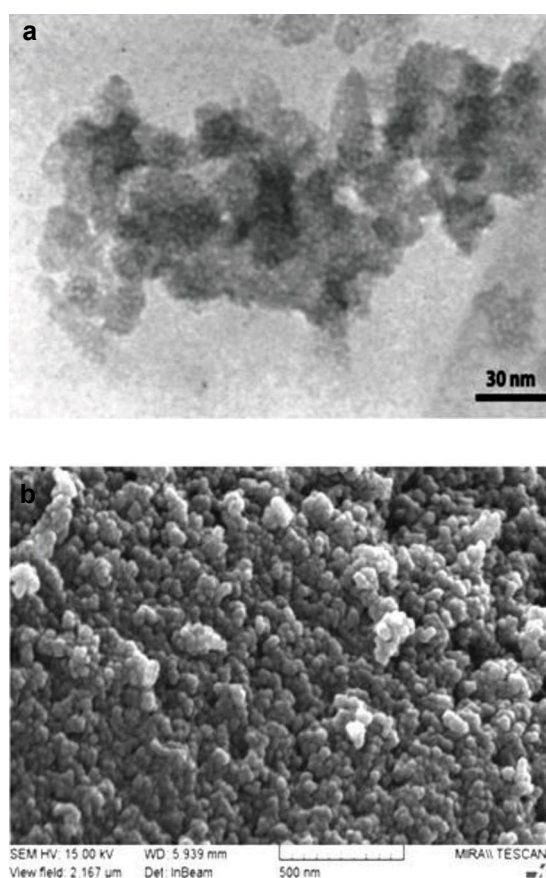


Fig. 5. (a) TEM image UVM-7 (b) SEM image UVM-7.

Effect of PH on MB adsorption

MB is a cationic dye, and therefore, surface charge on the adsorbent in the absorption of MB is very important. The adsorptive removal of solution during the adsorption process mainly depends on solution pH, since it affects both the ionization degree and surface property of the adsorbents.

Figure 6 depicts the effect of pH on the MB adsorption. It was found that the adsorption capacity increased with increasing pH values. This can be found by considering the electrostatic attraction between the negative charges of the adsorbent surface that leads to the absorption of cationic dye MB. In other words, by increasing the pH, OH ions increase and thereby increases absorption of positive ions on the adsorbent surface [21]. In UVM-7/SO₃H Due to the presence of SO₃⁻, the negative charges adsorbent surface enhances that result increased absorption.

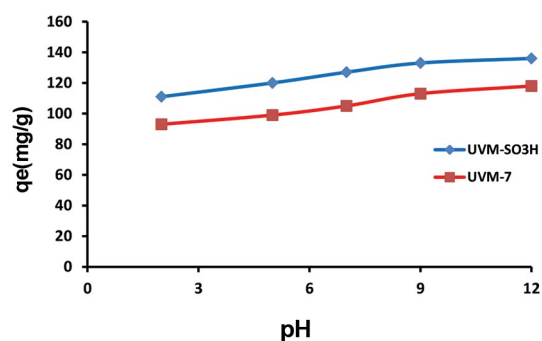


Fig. 6. Effect of pH on removal of MB.

Effect of temperature on MB adsorption

The effect of temperature on the adsorption of MB is shown in Figure 7. The results revealed that the adsorption capacity increases with increasing temperature, showing that this process is endothermic. The increased adsorption capacity with temperature may be attributed to increase the rate of diffusion of the adsorbent across the external boundary layer and in the internal pores

of the adsorbent particle, owing to the decrease in the viscosity of solution [22].

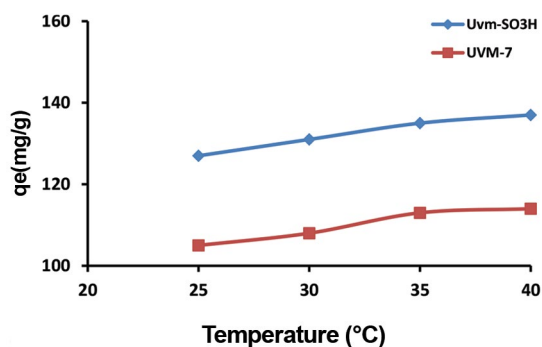


Fig. 7. Effect of temperature on removal of MB.

In order to gain an insight into the mechanism involved in the adsorption process, thermodynamic parameters for the present system were calculated. The adsorption free energy (ΔG), adsorption enthalpy (ΔH) and adsorption entropy (ΔS) from the Langmuir isotherms at different temperatures were calculated using the following thermodynamic functions:

$$\ln kc = \frac{-\Delta H}{RT} + \frac{\Delta S}{R} \quad (2)$$

The slope and intercept of the van't Hoff plot is equal to $-\Delta H/R$ and $\Delta S/R$, respectively, where R is the universal gas constant (8.314 J (molK)); T is the absolute temperature (K) [23,24]. The change in standard free energy (ΔG) of adsorption was

calculated from the following equation:

$$\Delta G = -RT \ln Kc \quad (3)$$

Where R is gas constant, K the equilibrium constant obtained from Langmuir equations and T is temperature in Kelvin. Thermodynamic parameters obtained are summarized in Table 2. It is noted that all ΔG values listed in Table 2 are negative. This suggests that the adsorption process is spontaneous. As seen from Table 2, the positive value of adsorption enthalpy shows that the adsorption process is endothermic.

The effect of salt concentration

The effect of various concentrations of NaCl and CaCl_2 solution on the amount of MB adsorbed onto per unit mass of UVM-7/ SO_3H for an initial MB concentration of 200 mgL^{-1} and adsorbents dose of 10 mg is shown in Figure 8. The wastewater containing dye has commonly higher salt concentration, and effect of ionic strength (or salt concentration) is of some importance in the study of dye adsorption onto adsorbents. From Figure 8, NaCl and CaCl_2 existed in solution affected the MB adsorption. It was seen that the increase in the salt concentration resulted in a decrease of MB adsorption. This trend indicated that the adsorbing efficiency decreased when NaCl and CaCl_2 concentration increased in the MB solution, which could be attributed to the competitive effect between MB ions and cations from the salt for the sites available for the adsorption process. As Ca^{+2} has more ionic strength and more positive charge than Na^+ so the effect of Ca^{+2} on adsorption MB is more serious than Na^+ .

Table 2. Thermodynamic parameters for the adsorption of MB on UVM-7 and UVM-7/ SO_3H as a function of temperature

T(K)	UVM-7			UVM-7/ SO_3H		
	$\Delta H(\text{kJ/mol})$	$\Delta G(\text{kJ/mol})$	$\Delta S(\text{kJ/mol K})$	$\Delta H(\text{kJ/mol})$	$\Delta G(\text{kJ/mol})$	$\Delta S(\text{kJ/mol K})$
298	12.6	-3.91	0.053	17.26	-7.14	0.0742
303	12.6	-4.56	0.053	17.26	-9.6	0.0742
308	12.6	-7.23	0.053	17.26	-11.37	0.0742
313	12.6	-8.26	0.053	17.26	-12.5	0.0742

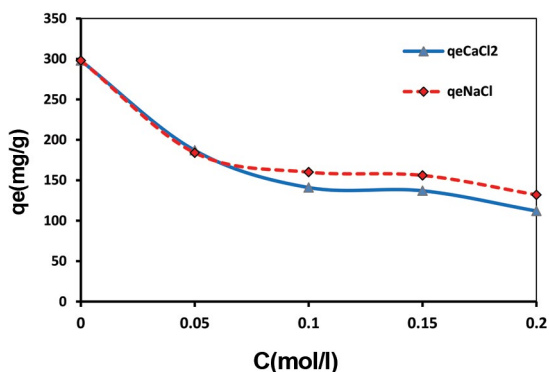


Fig. 8. effect of salt concentration on removal of MB.

Effect of contact time

The effect of contact time on the adsorption of MB is shown in Figure 9. The rapid adsorption rate at the beginning of adsorption process may be explained by the increase number of active sites on the sorbent surface, which would result in an increased concentration gradient between sorbent in the solution and on the sorbent surface. It can be seen that the adsorption after 80 min, the amount will not increase significantly; the absorption rate is controlled by the transfer of dye adsorbed on the surface of the adsorbent into the adsorbent particles. Therefore, to study the kinetics and adsorption isotherms, duration 80 min as the time required to reach equilibrium is considered.

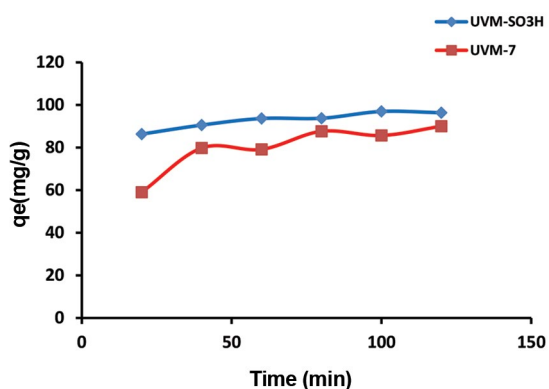


Fig. 9. Effect of contact time on removal of MB.

Effect of initial dye concentration

The experiments conducted with 0.01g of adsorbent, 10 ml of dye solution. Figure 10 shows the effects of initial concentration on the adsorption MB that shows the adsorption of MB increases with

an increase in the initial concentration (50, 100, 150, 200 mg/g). This phenomenon was due to the fact that when the initial concentration increases; the mass transfer driving force became larger, hence resulting in higher MB adsorption.

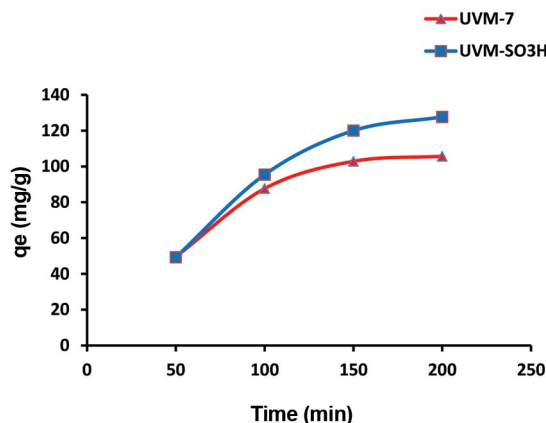


Fig. 10. Effect of initial concentration on removal MB.

Adsorption isotherms

In general, an adsorption isotherm is an invaluable curve describing the phenomenon governing the retention or mobility of a substance from the aqueous media or aquatic environment to a solid -phase at a constant temperature and PH [25, 26]. Study of equilibrium of adsorption isotherms provide information on the capacity of the adsorbent and play an important role in understanding the mechanism of adsorption. Several isotherm models are presented. Langmuir and Freundlich models are the most widely used to describe the adsorption isotherm.

Langmuir adsorption isotherm model to MB adsorption

Langmuir isotherm describes quantitatively the formation of a monolayer adsorbent on the outer surface of the adsorbent, and after that no further adsorption takes place. The model assumes uniform energies of adsorption onto the surface and no transmigration of adsorbent in the plane of the surface and the maximum adsorption capacities for each dye was calculated using the Langmuir adsorption model that can be summarized by the following equation [27, 28]:

$$\frac{C_e}{q_e} = \frac{1}{b q_m} + \frac{C_e}{q_m} \tag{4}$$

Where C_e (mg/L) is the equilibrium concentration, q_e (mg/g) the amount of adsorbent adsorbed per unit mass of adsorbent, and q_m is a constant that reflects the maximum adsorption capacity and b is a direct measure of the intensity of the adsorption process that is related to the heat of adsorption (L/mg). The essential features of the Langmuir isotherm can be expressed in terms of a dimensionless constant separation factor (R_L), which is defined by the following relationship:

$$R_L = \frac{1}{1 + bC_0} \quad (5)$$

According to the value of R_L , the isotherm shape may be interpreted as follows [29]:

- $R_L > 1.0$ Unfavorable
- $R_L = 1.0$ Linear
- $1 > R_L > 0$ Favorable
- $R_L = 0$ Irreversible

Freundlich adsorption isotherm model to MB adsorption

The empirical Freundlich model gives an expression encompassing the surface heterogeneity and exponential distribution of active sites and their energies, which is commonly presented as follows [30-32]:

$$\log q_e = \log K_F + 1/n \log C_e \quad (6)$$

Where K_F is the Freundlich constant and $1/n$

is the heterogeneity factor. The slope $1/n$ ranging between 0 and 1 is a measure of adsorption intensity or surface heterogeneity, becoming more heterogeneous as its value gets closer to zero.

The Langmuir and Freundlich parameters for adsorption of MB are listed in Table 3, indicating that the Langmuir isotherm model yielded the best fit with the highest R^2 value.

Adsorption kinetic study

The kinetic behavior of the adsorption process was studied under the temperature of 24.5 ± 0.5 °C and pH 6.3 using different initial dye concentrations (50, 100, 150, 200 mg/L). The controlling mechanisms of adsorption process such as chemical reaction, diffusion control or mass transfer coefficient are used to determine kinetic models. In this respect, the pseudo-first-order model and pseudo-second-order model were used to test the experimental data of different initial concentration [33, 34].

Application of pseudo-first-order model on MB adsorption

The pseudo-first-order kinetic model has been widely used to predict dye adsorption kinetics. The pseudo-first-order model was described by the following equation [35]:

$$\frac{1}{q_t} = \frac{k_1}{q_e} \left(\frac{1}{t}\right) + \frac{1}{q_e} \quad (7)$$

Where q_e and q_t are the adsorption capacities (mg/g) at equilibrium and at time t , respectively, k_1 is the rate constant of pseudo-first order adsorption (L/min).

Table 3. Isotherm parameters for adsorption of MB

adsorbent	Langmuir					Freundlich		
	q_m (mg/g)	b (L/mg)	R^2	K_L	R_L	K_F (mg/g(L/mg) ^{1/n})	N (L/mg)	R^2
UVM-7	107.5	0.6	0.99	6.54	0 < R_L < 1	57.3	6.8	0.98
UVM-7/SO ₃ H	129.9	0.0611	0.99	79.63	0 < R_L < 1	59.1	5	0.91

Table 4. Kinetic parameters of adsorption of MB on UVM-7 and UVM-7/SO₃H

adsorbent	pseudo-first-order kinetic			pseudo-second-order kinetic		
	q _e (mg/g)	K ₁ (L/min)	R ²	q _e (mg/g)	K ₂ (g/(mg.min))	R ²
UVM-7	42.2	0.03	0.912	101	0.0007	0.99
UVM-7/SO ₃ H	15.6	0.03	0.917	99	0.003	0.99

Application of pseudo-second-order model on MB adsorption

The pseudo-second-order model was applied to predict the adsorption behavior during the entire adsorption period and is in accordance with the adsorption mechanism of rate controlling steps. The pseudo-second-order model was described by the following equation [36]:

$$\frac{t}{q_t} = \frac{1}{k_2 q_e^2} + \frac{1}{q_e} t \quad (8)$$

Where q_e is the equilibrium adsorption capacity, and K₂ is the pseudo- second-order constants (g/mg min) can be determined experimentally from the slope and intercept of plot t/q_t versus t, is a straight line as shown in Figure 11.

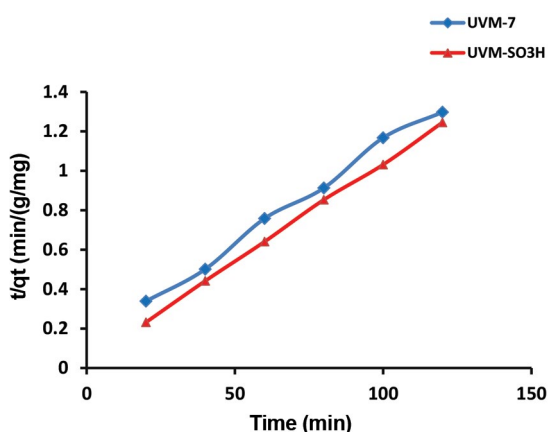


Fig. 11. pseudo-second-order kinetic on removal MB.

The experimental and calculated parameters of the kinetic equations above are summarized in Table 4, These results suggest that the adsorption of

MB dyes be best described by the pseudo-second-order kinetic model at all temperatures with high correlation coefficients.

CONCLUSION

The present study shows that UVM-7 and UVM-7/HO₃ is an effective adsorbent for the removal of methyl blue from aqueous solution. Several adsorption conditions such as PH, initial dye concentration, salt concentration, contact time and the temperature will influence its adsorption capacity for MB. It was found that the adsorption isotherm data fitted well with the Langmuir models, suggesting the adsorption to be monolayer and physical in nature. The kinetic data indicates that the pseudo-second order kinetic model was found to be well suited and highly correlated with the experimental data in the adsorption process.

CONFLICT OF INTEREST

The authors declare that there is no conflict of interests regarding the publication of this manuscript.

REFERENCES

1. S. Kaur and V. Singh. TiO₂ mediated photocatalytic degradation studies of Reactive Red 198 by UV irradiation. *J.hazardous.mater.*, 141(1) 230-236 (2007).
2. H. Nadi, M. Alizadeh, M. Ahmadabadi, A.R. Yari and S. Hashemi. Removal of Reactive Dyes (Green, Orange, and Yellow) from Aqueous Solutions by Peanut Shell Powder as a Natural Adsorbent. *Archives. Hygiene. Sciences.*, 1 (2012).
3. M. H .Entezari, Z. Sharif Al-Hoseini and N. Ashraf. Fast and efficient removal of Reactive Black 5 from aqueous solution by a combined method of ultrasound and sorption process. *Ultra.sono.chem.*, 15 (4) 433-437(2008).
4. Crini, Gregorio. Non-conventional low-cost adsorbents for dye removal: a review. *Bioresource. techno.*, 97(9)1061-1085(2006).
5. V. Vadivelan and K. V. Kumar. Equilibrium, kinetics, mechanism, and process design for the sorption of methylene blue onto rice husk. *J. Colloid and Interface. Science.*, 286 (1)90-100 (2005).

6. K. Kumar, V. Vasanth, S. Ramamurthi and Sivanesan. Modeling the mechanism involved during the sorption of methylene blue onto fly ash. *J. Colloid and Interface. Science.*, 284(1) 14-21(2005).
7. P. Thongchai and S. Wongchaisuwan. Mechanisms of dye wastewater colour removal by magnesium carbonatehydrated basic. *Water Science & Techno.*, 18(3)139-144(1986).
8. P.K. Malik and S.K. Saha. Oxidation of direct dyes with hydrogen peroxide using ferrous ion as catalyst. *Separ and purific. techno.*, 31(3)241-250(2003).
9. M. Koch. Ozonation of hydrolyzed azo dye reactive yellow 84 (CI). *Chemosphere* 46., 1(1)109-113(2002).
10. Ciardelli, Gianluca, L. Corsi, and M. Marcucci. Membrane separation for wastewater reuse in the textile industry. *Resources, conservation and recycling.*, 31(2)189-197(2001).
11. W. Feng-Chin and R Tseng. High adsorption capacity NaOHactivated carbon for dye removal from aqueous solution. *J. hazardous materials.*, 152(3)1256-1267(2008).
12. N. Thinakaran and et al. Removal of Acid Violet 17 from aqueous solutions by adsorption onto activated carbon prepared from sunflower seed hull. *J. hazardous materials.*, 151 (2)316-122(2008).
13. V. Gomez, M.S. Larrechi and M.P . Callao. Kinetic and adsorption study of acid dye removal using activated carbon. *Chemosphere.*, 69 (7)1151-1158(2007).
14. Z. Mao-Xu and et al. Removal of an anionic dye by adsorption/ precipitation processes using alkaline white mud. *J. Hazardous Materials.*, 149 (3)735-741(2007).
15. N.A. Khan ,Z. Hasan and S. H. Jhung. Adsorptive removal of hazardous materials using metal-organic frameworks (MOFs): A review. *J. hazardous materials.*, 244.444-456 (2013).
16. Y. Shao, X. Wang, Y. Kang, Y. Shu and Q. Li, L. Sun. Application of Mn/MCM-41 as an adsorbent to remove methyl blue from aqueous solution. *J. colloid and interface science.*, 429.25-33(2014).
17. A. Gil, F.C.C. Assis, S. Albeniz and S.A. Korili. Removal of dyes from wastewaters by adsorption on pillared clays. *J. Chem.Engin.*, 168(3)1032-1040(2011).
18. F.A. Pavan , A.C. Mazzocato and Y. Gushikem. Removal of methylene blue dye from aqueous solutions by adsorption using yellow passion fruit peel as adsorbent. *Bioresource Technology.*, 99(8)3162-3165(2008).
19. C. Gao, Y. Sakamoto, K. Sakamoto, O. Terasaki and S. Che. Synthesis and Characterization of Mesoporous Silica AMS-10 with Bicontinuous Cubic P6mm Symmetry. *Angewandte Chemie International Edition.*, 45(26)4295-4298(2006).
20. W.Li, Q.Yue, Y. Deng and D.Zhao. Ordered Mesoporous Materials Based on Interfacial Assembly and Engineering. *Advanced Materials.*, 25(37)5129-5152(2013).
21. S. Barma and B. Mandal. Synthesis and characterization of ordered mesoporous silica membrane: Role of porous support and gas permeation study. *Micro. Meso Materials.*, 210.10-19(2015).
22. O. Gulnaz, A. Sahnurova and S. Kama. Removal of Reactive Red 198 from aqueous solution by *Potamogeton crispus*. *J.Chem. Engin.*, 174(2)579-585(2011).
23. M. Anbia and S.A. Hariri. Removal of methylene blue from aqueous solution using nanoporous SBA-3. *Desalination.*261(1)61-66(2010).
24. O. Yunus. Kinetics of adsorption of dyes from aqueous solution using activated carbon prepared from waste apricot. *J. hazardous materials.*, 137(3)1719-1728(2006).
25. S.A. Karaca, M. Gurses and Ejder M. Acikyildiz. Adsorption of cationic dye from aqueous solutions by activated carbon. *Micro. Meso. Materials.*, 115(3)378-382(2008).
26. G. Limousin. Sorption isotherms: a review on physical bases, modeling and measurement. *Applied Geochemistry.*, 22(2)249-275(2007).
27. S.J. Allen , G. McKay and J.F. Porter. Adsorption isotherm models for basic dye adsorption by peat in single and binary component systems. *J. Colloid. Interface. Science.*, 280(2)322-333(2004).
28. G.H. Ghanizadeh and G.H.Asgari. Removal of methylene blue dye from synthetic wastewater with bone char. *J. Health. Environment.*, 2(2)104-113(2009).
29. M.C .Cibi, B. Mahjoub and M. Seffen. Adsorptive removal of textile reactive dye using *Posidonia oceanica* fibrous biomass. *J. Environmental Science. Technology.*, 4(4)433-444(2007).
30. N.K.Amin. Removal of reactive dye from aqueous solutions by adsorption onto activated carbons prepared from sugarcane bagasse pith. *Desalination.*, 223.152-161(2008).
31. N.A. Oladoja, C.O. Aboluwoye and A.O. Akinkugbe. Evaluation of loofah as a sorbent in the decolorization of basic dye contaminated aqueous system. *Industrial. Engin. Chemistry.*, 48(6)2786-2794(2009).
32. M.R. Mehrasbi. Heavy metal removal from aqueous solution by adsorption on modified banana shell. *J. Health. Environment.*, 1(1)57-66(2008).
33. J.P. Silva, S. Sousa, J. Rodrigues, H. Antunes , J.J. Porter, I. Goncalves and S. Ferreira-Dias. Adsorption of acid orange 7 dye in aqueous solutions by spent brewery grains. *Separ . Purific. Techno.*, 40(3)309-315(2009).
34. H. Yuh-Shan. Review of second-order models for adsorption systems. *J. hazardous materials.*136(3)681-689(2006).
35. E. Repo, J.K. Warchol. A. Bhatnagar and M. Sillanpaa. Heavy metals adsorption by novel EDTA-modified chitosan-silica hybrid materials. *J. colloid. interface science.*, 358(1)261-267(2011).
36. Y. Shao, X. Wang, Y. Shu, Q. Sun and L. Li. Application of Mn/MCM-41 as an adsorbent to remove methyl blue from aqueous solution. *J. colloid and interface science.*, 429.25-33(2014).
37. Y.S.Ho and G. McKay. Pseudo-second order model for sorption processes. *Process biochemistry.*, 34(5)451-465(1999).